

Kondo-lattice formation in cubic-phase YbCu₅

N. Tsujii, J. He, F. Amita, K. Yoshimura, and K. Kosuge

Division of Chemistry, Graduate School of Science, Kyoto University, Kyoto 606-01, Japan

H. Michor and G. Hilscher

Institute für Experimentalphysik, Technische Universität Wien, Wiedner Hauptstrasse 8-10, A-1040 Wien, Austria

T. Goto

Institute for Solid State Physics, University of Tokyo, Roppongi-7, Minato-ku, Tokyo 106, Japan

(Received 5 May 1997)

The YbCu₅ phase with *C15b* structure has been prepared by a high-pressure technique, and its physical properties have been investigated. The temperature dependence of magnetic susceptibility, electrical resistivity, and specific heat show Kondo-lattice formation. Furthermore, a heavy Fermi-liquid state without magnetic ordering down to 2.0 K is found to evolve below about 6 K. The electronic specific heat coefficient γ is enhanced to values as large as to 550 mJ/mol K². The magnetization measured up to 40 T at 1.6 K has a field dependence which is expected for a Kondo system when the total angular momentum is $J > 1$. All results are in good agreement with the extrapolation of the previous results of YbCu_{5-x}Ag_x ($0.125 \leq x \leq 1.0$) for $x \rightarrow 0$. The concentration dependence of characteristic temperatures of YbCu_{5-x}Ag_x can be quantitatively explained by the chemical pressure effect within the compressible Kondo model for the full range of Ag concentration ($0.0 \leq x \leq 1.0$). The origins of Kondo-lattice formation in YbCu₄Ag and the valence transition in YbCu₄In are discussed. [S0163-1829(97)88837-0]

I. INTRODUCTION

The YbCu₄*M* (*M*=In, Ag, Au, Pd) compounds crystallize in the cubic AuBe₅-type (*C15b*) structure and preserve the Yb ion in its trivalent state with total angular momentum $J=7/2$.^{1,2} These systems have been investigated extensively because of their rich variety of phenomena at low temperatures. For instance, YbCu₄In exhibits a sharp valence transition at $T_v \approx 40$ K, suggested by its abrupt change of magnetic susceptibility from a Curie-Weiss behavior above T_v into an enhanced Pauli paramagnetism below T_v .³ It was shown that this valence transition is also induced by a magnetic field around $H_m \approx 40$ T at 4.2 K.⁴ The low-temperature and low-field state is well described by the Fermi-liquid behavior, as is shown by the Korringa-type relaxation in the ⁶³Cu nuclear quadrupole (NQR) and ¹¹⁵In NMR experiments.^{5,6} As for YbCu₄Ag, this system is known to be a typical dense Kondo system with a moderately large electronic specific heat coefficient $\gamma \approx 200$ mJ/mol K².^{2,7} Furthermore, the temperature dependence of magnetic susceptibility² and the magnetic term of specific heat⁸ are well accounted for by the Bethe-ansatz solution of the Coqblin-Schrieffer model.⁹ Neutron studies give no evidence of crystal-field excitations at low temperature.¹⁰ On the other hand, the Kondo effect is not dominant in YbCu₄Au and YbCu₄Pd, and long-range magnetic ordering is observed at 0.6 and 0.8 K, respectively.² Especially for YbCu₄Au, well-defined crystal-field excitations are observed by neutron-scattering experiments.¹⁰

Such a variety of properties for YbCu₄*M* compounds motivated us to investigate the YbCu₅ compound, which is thought to be a mother compound of YbCu₄*M* systems. Previously YbCu₅ was reported to have the hexagonal CaCu₅-type structure, not the cubic AuBe₅-type, and to be

nonmagnetic with a closed *4f* shell (*4f*¹⁴) of the divalent Yb ion.¹¹ Lately, Hornstra and Buschow suggested that the precise chemical composition of the hexagonal CaCu₅-type phase is YbCu_{6.5}.¹² This has been accepted until today, and the YbCu₅ phase has not appeared to exist in the binary Yb-Cu phase diagram. Recently, however, it has been revealed that the YbCu₅ compound with the cubic AuBe₅ structure exists and can be stabilized under high pressure.¹³ Furthermore, cubic YbCu₅ is found to have the trivalent Yb ion with total angular momentum $J=7/2$. Therefore, cubic YbCu₅ can be regarded as the *real* mother compound of YbCu₄*M* systems from the viewpoints of both structure and the valence of Yb. Thus it is of great interest to investigate in detail the properties of cubic YbCu₅, because the electronic state of cubic YbCu₅ will shed light on the origin of the anomalous phenomena of YbCu₄*M* compounds.

Recently, we have reported on the structural and physical properties of YbCu_{5-x}Ag_x, the solid solution system between YbCu₄Ag and YbCu₅.¹⁴ The results reveal that cubic YbCu_{5-x}Ag_x compounds are obtained as single-phase specimens for a wide range of Ag concentration x ($0.125 \leq x \leq 1.0$) and form a series of dense Kondo systems in which a nonmagnetic Fermi-liquid state develops at low temperatures and the Kondo temperature decreases with decreasing concentration x . Furthermore, the concentration dependence of the quadratic term of the temperature dependence of resistivity, A , is well explained by the chemical pressure effect upon YbCu₄Ag, suggesting that the electronic structure of YbCu_{5-x}Ag_x is unchanged by the Cu substitution. This fact seems to imply that cubic YbCu₅ is also a dense Kondo compound with a Fermi-liquid ground state. From an extrapolation of $x \rightarrow 0$, cubic YbCu₅ is anticipated to have a heavy-fermion state characterized by $\gamma \approx 500$ mJ/mol K², a

value close to that of $\text{YbCu}_{4.5}$, $\gamma \approx 600 \text{ mJ/mol K}^2$,¹⁵ which is so far the heaviest fermion state among the Yb-based systems with a nonmagnetic ground state.¹⁶ However, $\text{YbCu}_{4.5}$ has such a complicated crystal structure, with 7448 atoms per unit cell,¹⁷ that band-structure calculations based on this unit cell might be difficult. Therefore, cubic YbCu_5 is also expected to be a very suitable Yb-based compound both for the model calculation and for the comparison with Ce- and U-based heavy-fermion compounds

II. EXPERIMENT

The sample of cubic YbCu_5 was prepared in two stages: arc melting and subsequent annealing under high pressure. When we started from the stoichiometric mixture of Yb:Cu = 1:5, we always find that the product is not a simple cubic- AuBe_5 -type phase, but is likely to be the deformed- AuBe_5 phase, similar to $\text{YbCu}_{4.5}$.¹⁷ Then we selected the nominal composition as $\text{YbCu}_{5+\delta}$ with $\delta=0.75$, using excess Cu. Metals of 99.99% pure Cu and 99.99% pure Yb were melted in an arc furnace under argon atmosphere. The x-ray-diffraction (XRD) pattern of the arc-melted sample (as-cast sample) showed that it was in a two-phase mixture, the deformed- AuBe_5 -type $\text{YbCu}_{4.5}$ and the hexagonal- CaCu_5 -type $\text{YbCu}_{6.5}$. Then, the as-cast sample was placed in a BN cell, annealed under the pressure of 1.5 GPa at 900 °C for 1 h, and then quenched to room temperature where the pressure was released. XRD shows the pattern of the cubic- AuBe_5 -type (C15b) phase and fcc Cu, without any other phase. The sample was subsequently sealed in an evacuated silica tube and annealed at ambient pressure at 350 °C for 20 days. X-ray diffraction confirmed that the compound maintained the cubic structure. When the sample was annealed at ambient pressure above 400 °C, the XRD pattern shows the patterns of two phases, $\text{YbCu}_{4.5}$ and $\text{YbCu}_{6.5}$, as observed for the as-cast sample. The sample composition was analyzed by the energy dispersive x-ray spectroscopy (EDS) using a scanning electron microscope (SEM). The results showed that the composition of the sample for this report is close to $\text{YbCu}_{5.6}$. Furthermore, the EDS analysis revealed that the cubic- AuBe_5 -type phase exhibits a homogeneous composition range from about $\text{YbCu}_{5.6}$ to $\text{YbCu}_{4.5}$. However, hereafter we describe the cubic phase simply as “cubic YbCu_5 ,” and the detailed phase diagram of the Yb-Cu system under high pressure and the composition dependence of the physical properties will be reported elsewhere. The lattice constant of cubic YbCu_5 was estimated from the XRD pattern by the least-squares method. Magnetic susceptibility was measured from 2 to 300 K by a superconducting quantum interference device (SQUID) magnetometer. Magnetization measurement was carried out by an induction method in a pulsed high magnetic field up to 40 T at 1.6 K. Electrical resistivity measurements were performed from 4.2 to 300 K by the conventional four-probe method. The specific heat was measured by a quasiadiabatic step-heating method in the temperature range from 2 to 80 K.

III. RESULTS AND DISCUSSION

In Fig. 1 is shown the XRD pattern of cubic YbCu_5 . The (200) reflection clearly appears. Therefore, cubic YbCu_5 is

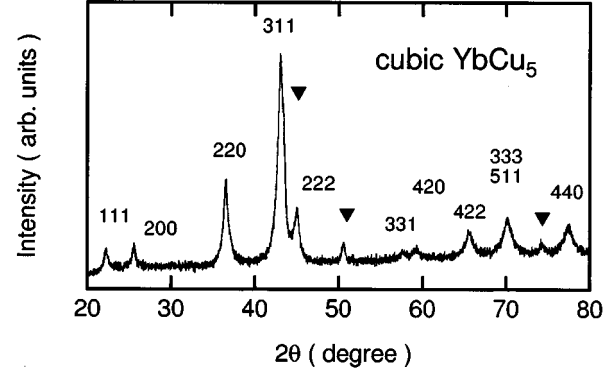


FIG. 1. Powder x-ray-diffraction pattern of cubic YbCu_5 . ▼ represents the diffraction from Cu metal.

found to have the ordered C15b-type structure, the same structure as the YbCu_4M ($M=\text{In, Ag, Au, Pd}$) system. From this pattern, the lattice constant is estimated to be 6.975 Å.

In Fig. 2, the temperature dependence of magnetic susceptibility χ and the inverse $1/\chi$ of cubic YbCu_5 are shown. Because the susceptibility of Cu metal is more than two orders of magnitude smaller than the scale in Fig. 2, the influence of the excess Cu can be ignored. Above 50 K, the data are well described by a Curie-Weiss law. The effective magnetic moments μ_{eff} is estimated to be $4.55\mu_B$, very close to the value $4.54\mu_B$, which is expected for a free Yb^{3+} ($J=7/2$) ion. The Weiss temperature Θ is evaluated to be -25 K. Below about 20 K, data deviate from the Curie-Weiss law with decreasing temperatures, pass through a maximum at $T_{\text{max}} \approx 10$ K, and then decrease below about 5 K. This behavior is similar to that of dense Kondo systems with a Fermi-liquid ground state such as YbCuAl ,¹⁸ CeRu_2Si_2 ,¹⁹ and YbCu_4Ag .² We should mention that the χ_{max} was not observed in our previous investigation for cubic YbCu_5 ,¹³ which might be due to the composition dependence. The value of $T_{\text{max}} \approx 10$ K is lower than those of $\text{YbCu}_{5-x}\text{Ag}_x$ ($0.125 \leq x \leq 1.0$) systems, where T_{max} is lowered from 42 K for $x=1.0$ to 15 K for $x=0.125$ and T_K is also reduced with the decrease of the Ag concentration x .¹⁴ Therefore, these χ - T data indicate that cubic YbCu_5 forms a Kondo-lattice state and the characteristic temperature of the Kondo effect is further reduced than that of $\text{YbCu}_{4.875}\text{Ag}_{0.125}$. According to the Bethe-ansatz solution of the Coqblin-Schrieffer model, the physical properties of a Kondo lattice are well scaled by the single energy parameter T_0 .⁹ With this model, Rajan showed that the susceptibility at 0 K, $\chi(0)$, is related to the characteristic temperature T_0 as

$$\chi(0) = N_A v (v^2 - 1) g_J^2 \mu_B^2 / 24 \pi k_B T_0, \quad (1)$$

where N_A is Avogadro's number, v the degeneracy of the ground state, g_J the Landé g factor, and k_B Boltzmann's constant. From Fig. 2, $\chi(0)$ is estimated to be 0.0475 emu/mol by subtracting the Curie term below about 5 K. This value gives the characteristic temperature $T_0 = 69.7$ K using $v=8$ and $g_J=8/7$. Rajan also calculated the temperature dependence of susceptibility based on the model, which is scaled by T_0 . However, as is shown in Fig. 2, the theoretical

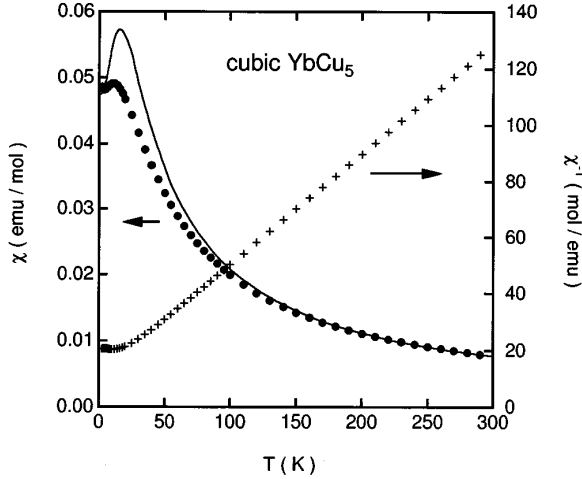


FIG. 2. Temperature dependence of magnetic susceptibility of cubic YbCu₅ and its inverse. The solid line represents the calculation based on the solution of the Coqblin-Schrieffer model (see text).

curve of $\chi(T)$ based on Rajan's calculation with $T_0=69.7$ K and $\chi(0)=0.0475$ emu/mol does not reproduce the experimental results well, especially the value of χ_{\max} , though the value of T_{\max} is very reasonable. Similar deviation between the theory and experimental data is also observed for YbCu_{4.875}Ag_{0.125}.²⁰ According to Ref. 9, the rate $\chi_{\max}/\chi(0)$ depends on the total angular momentum J , and decreases from about 1.25 for $J=7/2$ to 1.0 for $J=1/2$. Therefore, the $\chi_{\max}/\chi(0)$ value is likely to become smaller than expected for $J=7/2$ when the crystalline-field effect is strong so that it reduced the eight-fold degeneracy of $J=7/2$ in Yb³⁺ at low temperature.

The field dependence of magnetization M measured at 1.6 K and up to the field $H=40$ T and its derivative dM/dH are displayed in Fig. 3. The magnetization increases linearly with field up to about 10 T, then turns to an upward curvature, and shows a maximum in the dM/dH curve at $H_m \cong 17$ T, until it begins to saturate toward $4\mu_B$ for a free Yb³⁺ magnetic moment. The maximum of dM/dH is not likely to suggest the existence of antiferromagnetic ordering below H_m , since the Zeeman energy of $H_m \cong 17$ T corresponds to be about 11 K ($\cong \mu_B H_m / k_B$) in temperature, while no magnetic order is detected around this temperature. On the other hand, a very similar magnetization curve is observed for several typical dense Kondo or heavy-fermion systems such as CeRu₂Si₂,²¹ CeCu₆,²² and YbCu₄Ag.^{4,23} Such a behavior seems to be characteristic in a Kondo-lattice system with a Fermi-liquid ground state. According to the theoretical calculation based on the Coqblin-Schrieffer model, the dM/dH curve has a maximum when the ground-state degeneracy is larger than 2.²⁴ With this result of the calculation for the $J=7/2$ case, the magnetization data of cubic YbCu₅ were fitted and the fitted line was indicated as a dashed line in Fig. 3. Figure 3 shows a fairly good agreement with the data and the theoretical calculation for the $J=7/2$ case with energy parameter $T_1=1.42$ meV (T_1 is the char-

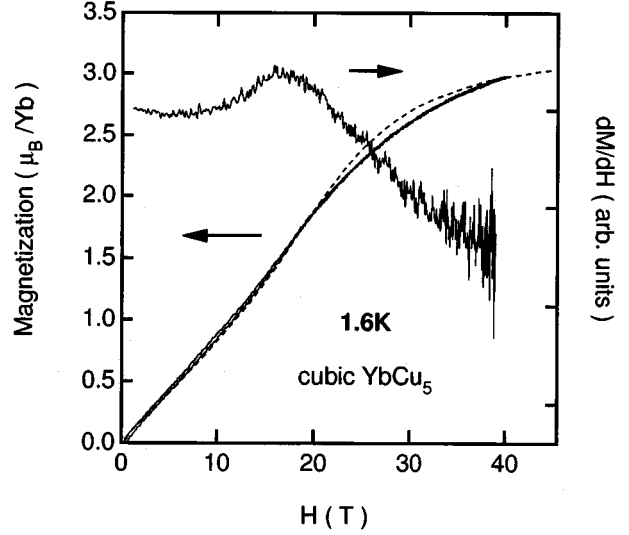


FIG. 3. Field dependence of magnetization of cubic YbCu₅ and its derivative dM/dH at 1.6 K. The dashed line represents the fit by the $J=7/2$ Coqblin-Schrieffer model (see text).

acteristic energy of the Kondo effect defined in Ref. 24). This value of T_1 yields the characteristic temperature $T_0=65.4$ K using the relations in Ref. 24, which is very close to the value $T_0=69.7$ K, estimated from the magnetic susceptibility data. Therefore, the ground state of cubic YbCu₅ is not a doublet, but very close to eight-fold, even though the degeneracy of Yb³⁺ is reduced by the crystal-field splitting.

In Fig. 4, the temperature dependence of electrical resistivity is shown. The absolute value of resistivity at room temperature is comparable to those of the YbCu_{5-x}Ag_x system.¹⁴ Therefore, we believe that the influence of the excess Cu is not significant. The resistivity decreases linearly from room temperature down to about 150 K, shows a minimum at $T_{\min} \cong 100$ K, and then increases slightly with decreasing temperature down to 30 K. This behavior is attributed to the single-site Kondo scattering caused by the localized $4f$ electron in the Yb³⁺ ion. T_{\min} is considered to be of the order of Kondo temperature T_K . At a further lowered temperature, the resistivity begins to decrease and shows a T^2 dependence below 6 K, as is evidenced by the inset of Fig. 4. This T^2 dependence is the characteristic of Kondo-lattice formation, in which $4f$ electrons behave as heavy quasiparticles at $T \ll T_K$. The T^2 coefficient A is derived to be $0.147 \mu\Omega \text{ cm K}^{-2}$.

In Fig. 5 is shown the specific heat C vs temperature T and C/T vs T^2 . No indication of magnetic order is observed down to 2.0 K. The electronic specific-heat coefficient is estimated to be as large as $\gamma \cong 550$ mJ/mol K² from a linear extrapolation of C/T to $T \rightarrow 0$. This large γ value is consistent with the extrapolation of the YbCu_{5-x}Ag_x series for $x \rightarrow 0$.¹⁴ According to the Bethe-ansatz solution of the Coqblin-Schrieffer model lead by Rajan,⁹ γ is universally scaled by the characteristic temperature T_0 as

$$\gamma = N_A(v-1)\pi k_B/6T_0. \quad (2)$$

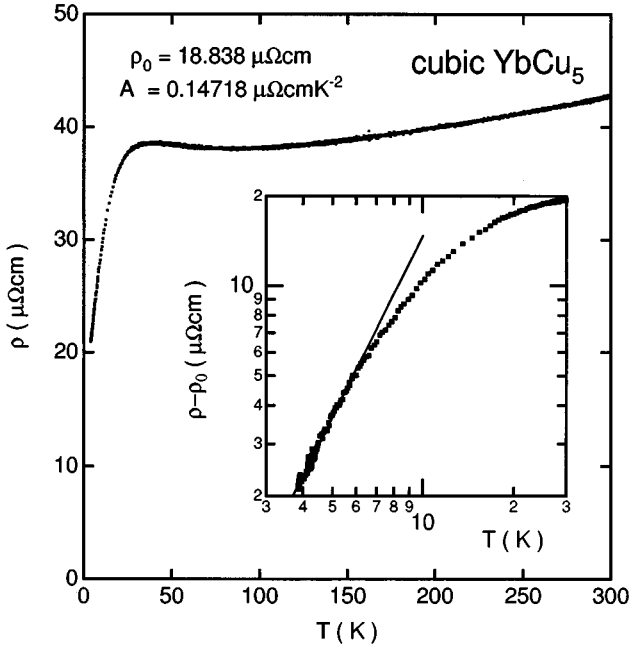


FIG. 4. Temperature dependence of electrical resistivity ρ of cubic YbCu_5 . The inset shows the log-log plot of $\rho - \rho_0$ (ρ_0 is the residual resistivity). The solid line indicates the T^2 dependence of the resistivity.

Using the degeneracy $\nu=8$, T_0 is evaluated to be 55.4 K through Eq. (2), close to the value of 69.7 K, estimated from the magnetic susceptibility data. On the other hand, our recent analysis of the specific heat indicates a reduction of the ground-state degeneracy of cubic YbCu_5 due to the crystal-field splitting, which would be of similar order of magnitude as T_0 .²⁵ However, a precise crystal-field scheme is not yet obtained and the effect of the crystal field cannot be taken into consideration quantitatively. Hence, for the above estimation of T_0 and the analysis of the susceptibility data, we assumed the ground-state degeneracy to be eight-fold. In order to solve this problem, neutron-scattering experiment should be performed.

There appears a maximum of C/T around $T^2 \approx 50 \text{ K}^2$. This peak is also seen in the data for heavy-fermion systems, such as CeCu_2Si_2 (Ref. 26) and CeCu_6 (Ref. 27) and is argued to be the consequence of the Abrikosov-Suhl resonance, giving rise to a pseudogap at the Fermi level.

In the previous paper, we reported that $\text{YbCu}_{5-x}\text{Ag}_x$ ($0.125 \leq x \leq 1.0$) is a series of Kondo-lattice systems of which the characteristic temperatures decrease with decreasing Ag concentration. This tendency was quantitatively accounted for by the chemical pressure effect.^{14,20} Since Yb^{3+} has a smaller ionic radius than the $\text{Yb}^{2+ \leftrightarrow 3+}$ intermediate-valent state, pressure stabilizes the magnetic Yb^{3+} state. This trend also appears to be value for $x=0$, i.e., cubic YbCu_5 . In the following, we discuss this within the compressible Kondo model.

The characteristic temperature T_0 is proportional to the Kondo temperature T_K , and so T_0 is described as

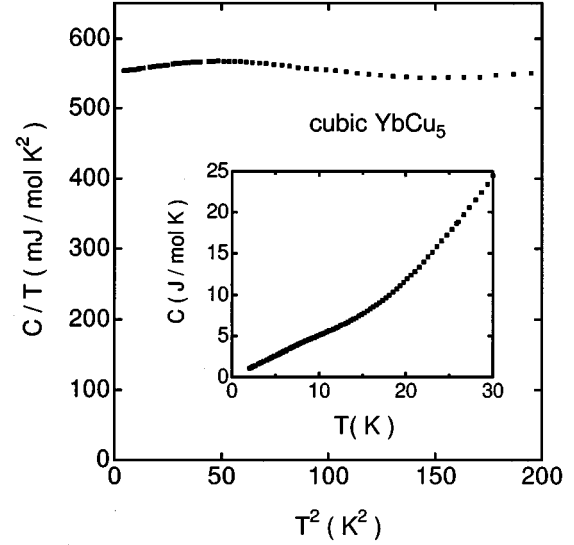


FIG. 5. Low-temperature specific heat of cubic YbCu_5 in a C/T vs T^2 plot. The inset shows C vs T .

$$T_0 \propto T_K \propto \exp\left[-\frac{1}{|JN(E_F)|}\right], \quad (3)$$

where J is the exchange interaction between conduction electron and $4f$ electron, and $N(E_F)$ is the density of states at the Fermi level. T_0 is evaluated from the susceptibility and the specific-heat data through the Eqs. (1) and (2), respectively, and is also evaluated from the T^2 coefficient of resistivity, A , as^{24,28}

$$T_0 \propto T_K \propto \frac{1}{\sqrt{A}}. \quad (4)$$

Now we assume that the value of $|JN(E_F)|$ for $\text{YbCu}_{5-x}\text{Ag}_x$ ($0.0 \leq x \leq 1.0$) depends only on the volume of the unit cell. In this case, the compressible Kondo model can be applied and $|JN(E_F)|$ of $\text{YbCu}_{5-x}\text{Ag}_x$ can be expressed as follows:²⁹

$$\begin{aligned} |JN(E_F)|_x &= |JN(E_F)|_1 \exp\left[-q \frac{V_x - V_1}{V_1}\right] \\ &\cong |JN(E_F)|_1 \left(1 - q \frac{V_x - V_1}{V_1}\right), \end{aligned} \quad (5)$$

where $|JN(E_F)|_x$ and $|JN(E_F)|_1$ are the value of $|JN(E_F)|$ for $\text{YbCu}_{5-x}\text{Ag}_x$ and YbCu_4Ag , q a coefficient, and V_x and V_1 the unit cell volumes for $\text{YbCu}_{5-x}\text{Ag}_x$ and for YbCu_4Ag , respectively. Since the volume change $V_x - V_1$ is found to be small from Ref. 14 and the present experiment, we have used

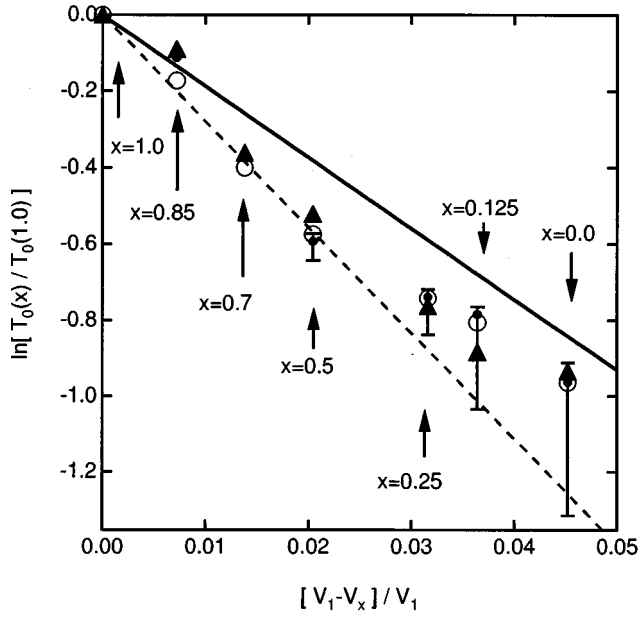


FIG. 6. $\ln[T_0(x)/T_0(1.0)]$ vs $(V_1 - V_x)/V_1$ for $\text{YbCu}_{5-x}\text{Ag}_x$ ($0.0 \leq x \leq 1.0$). ●, ○, and ▲ represent the data from the specific heat, the magnetic susceptibility, and the electrical resistivity, respectively. The solid and dashed lines stand for the predictions of the compressible Kondo model for YbCu_4Ag under hydrostatic pressure with $q/|JN(E_F)|_0 = -18.6$ and -27.8 kbar^{-1} , respectively (see text for details).

only the linear term in Eq. (5). Then from Eqs. (3), (4), and (5), we obtain the relations among T_0 , A , and V as

$$\ln \frac{T_0(x)}{T_0(1.0)} = -\frac{1}{2} \ln \frac{A_x}{A_1} = \frac{q}{|JN(E_F)|_1} \frac{V_1 - V_x}{V_1}, \quad (6)$$

where $T_0(x)$ and A_x are the characteristic temperature T_0 and the value of A for $\text{YbCu}_{5-x}\text{Ag}_x$, respectively. In Fig. 6 are displayed the values of $T_0(x)/T_0(1.0)$ as functions of $(V_1 - V_x)/V_1$. Here, T_0 was evaluated from the specific-heat,³⁰ the magnetic susceptibility, and the electrical resistivity data assuming the ground-state degeneracy to be eight-fold. The unit-cell volume of $\text{YbCu}_{5-x}\text{Ag}_x$ was already reported.¹⁴ The error bars are indicated for the specific-heat data, and errors of the same order should exist in the susceptibility and the resistivity data. These errors arise from the estimation of T_0 , because the crystal field reduces the degeneracy and would consequently reduce T_0 from those values of T_0 obtained by assuming an eight-fold degeneracy. Figure 6 clearly shows that the linear relation of Eq. (6) is valid for the full range of concentration x . Bauer *et al.* investigated the electrical resistivity of YbCu_4Ag under hydrostatic pressure up to 80 kbar, and obtained a $q/|JN(E_F)|_1$ value for YbCu_4Ag of about -18.6 and -27.8 kbar^{-1} , evaluated from the value of T_{max} and the coefficient A , respectively.³¹ In Fig. 6, the solid and dashed lines correspond to Eq. (6) using these values $q/|JN(E_F)|_1$, respectively. It is apparent that these lines trace our data quite well. A least-squares fitting to our data yields the value -21.8 kbar^{-1} for

$q/|JN(E_F)|_1$ of YbCu_4Ag , very close to that obtained by Bauer *et al.* This agreement indicates that the physical properties of $\text{YbCu}_{5-x}\text{Ag}_x$ are quantitatively explained simply by the chemical pressure effect, and the electronic structure is not changed qualitatively by Cu substitution. Therefore, the origin of the Kondo-lattice state in YbCu_4Ag with $\gamma \approx 200/\text{mol K}^2$ is attributed to the negative chemical pressure effect on cubic YbCu_5 . It is notable that the parameter q has a negative value for this case, showing a contrast with the case for Ce-based compounds^{32,33} in which q has a positive value and is usually taken to be between 6 and 8. If we assume $q = -6$ for our case, we obtain the $|JN(E_F)| = 0.201$ for cubic YbCu_5 through Eq. (6). This value is approximately 2 or 3 times larger than that of CeCu_6 (Ref. 32) and CeInCu_2 (Ref. 33) which show further heavy-fermion states than cubic YbCu_5 .

While YbCu_4Ag has a Kondo-lattice ground state, YbCu_4In shows a sharp valence transition at $T_v = 40 \text{ K}$. Recently, it has been reported that this valence transition is strongly affected and rapidly broadened by the disorder between In and Yb sites.³⁴ This indicates that the tetrahedral coordination of Yb atom with four In atoms in the ordered $C15b$ structure is necessary for the sharp valence transition, and therefore the chemical bonding between Yb $4f$ and In $5p$ levels is, at least partially, responsible for the transition. This is also confirmed by our recent results for the isostructural $\text{YbCu}_{5-x}\text{In}_x$ systems.³⁵ In this system, an In atom on a $4c$ site is replaced by a Cu atom, while the Yb sublattice preserves the face-centered-cubic structure, in contrast to a substitution like $\text{Yb}_{1-x}\text{In}_x\text{Cu}_2$. In $\text{YbCu}_{5-x}\text{In}_x$, the valence transition is rapidly broadened by a faint substitution of Cu. Furthermore, for the compounds of a small In concentration of $0.1 \leq x \leq 0.5$ a $\ln T$ dependence of resistivity is observed and a T^2 dependence is absent down to low temperatures. This suggests that the hybridization between Yb $4f$ and In $5p$ levels is so large, disturbing the coherent Kondo state in cubic YbCu_5 . As for YbCu_4Au and YbCu_4Pd , the origin of magnetic ordering and the absence of a Kondo-lattice state is still unknown. Solid-solution systems such as $\text{YbCu}_{5-x}\text{Au}_x$ etc., will give valuable information for this reason.

In conclusion, the physical properties of YbCu_5 with cubic AuBe_5 structure have been investigated. The results of magnetic susceptibility, electrical resistivity, and specific heat show the characteristic behavior of the Kondo lattice with a Fermi-liquid ground state. The characteristic temperature T_0 is estimated as 60 K, which is further reduced from that of $\text{YbCu}_{4.875}\text{Ag}_{0.125}$. The electronic specific-heat coefficient is as large as $\gamma \approx 550 \text{ mJ/mol K}^2$. The temperature dependence of the magnetic susceptibility does not agree well with the solution of the Coqblin-Schrieffer model. This deviation may be due to the crystal-field effect, which reduces the degeneracy of the total angular momentum $J = 7/2$ in the Yb^{3+} state. However, the field dependence of magnetization at 1.6 K has a maximum of dM/dH and shows fairly good agreement with calculation for the $J = 7/2$ Coqblin-Schrieffer model. This indicates that the ground state of cubic YbCu_5 is not a doublet and is very close to eight-fold degeneracy. The concentration dependence of T_0 for $\text{YbCu}_{5-x}\text{Ag}_x$ ($0.0 \leq x \leq 1.0$) is in good agreement with the pressure dependence for YbCu_4Ag and is well explained within the compressible

Kondo model. This result implies that the electronic structure of $\text{YbCu}_{5-x}\text{Ag}_x$ ($0.0 \leq x \leq 1.0$) is not changed qualitatively by Cu substitution. Therefore, the Kondo-lattice state in YbCu_4Ag with $\gamma \approx 200$ mJ/mol K^2 is attributed to a negative chemical pressure effect on cubic YbCu_5 . On the other hand, the valence transition in YbCu_4In cannot be explained by the chemical pressure, suggesting that the hybridization between Yb $4f$ and In $5p$ is important for the transition.

ACKNOWLEDGMENT

We are grateful to Professor Ernst Bauer for useful suggestions. We also thank M. Kato for a lot of help. Some of the authors (N.T., K.Y., and K.K.) also gratefully acknowledge Professor T. Kasuya for valuable suggestions. This work has been supported by a grant-in-aid for scientific research from the Ministry of Education, Science and Culture of Japan.

- ¹K. Kojima, H. Hayashi, A. Minami, Y. Kasamatsu, and T. Hihara, *J. Magn. Magn. Mater.* **81**, 267 (1989).
- ²C. Rossel, K. N. Yang, M. B. Maple, Z. Fisk, E. Zirngiebl, and J. D. Thompson, *Phys. Rev. B* **35**, 1914 (1987).
- ³I. Felner, I. Nowik, D. Vaknin, Ulrike Potzel, J. Moser, G. M. Kalvius, G. Wortmann, G. Schmiester, G. Hilscher, E. Gratz, C. Schmitzer, N. Pillmayr, K. G. Prasad, H. de Waard, and H. Pinto, *Phys. Rev. B* **35**, 6956 (1987).
- ⁴K. Yoshimura, T. Nitta, M. Mekata, T. Shimizu, T. Sakakibara, T. Goto, and G. Kido, *Phys. Rev. Lett.* **60**, 851 (1988).
- ⁵H. Nakamura, K. Nakajima, Y. Kitaoka, K. Asayama, K. Yoshimura, and T. Nitta, *J. Phys. Soc. Jpn.* **59**, 28 (1990).
- ⁶K. Yoshimura, T. Nitta, T. Shimizu, M. Mekata, H. Yasuoka, and K. Kosuge, *J. Magn. Magn. Mater.* **90-91**, 466 (1990).
- ⁷D. T. Adroja, S. K. Malik, B. D. Padalia, and R. Vijayaraghavan, *J. Phys. C* **20**, L307 (1987).
- ⁸M. J. Besnus, P. Haen, N. Hamdaoui, A. Herr, and A. Meyer, *Physica B* **163**, 571 (1990).
- ⁹V. T. Rajan, *Phys. Rev. Lett.* **51**, 308 (1983).
- ¹⁰A. Severing, A. P. Murani, J. D. Thompson, Z. Fisk, and C. -K. Loong, *Phys. Rev. B* **41**, 1739 (1990).
- ¹¹A. Iandelli and A. Palenzona, *J. Less-Common Met.* **25**, 333 (1971).
- ¹²J. Hornstra and K. H. J. Buschow, *J. Less-Common Met.* **27**, 123 (1972).
- ¹³J. He, N. Tsujii, M. Nakanishi, K. Yoshimura, and K. Kosuge, *J. Alloys Compd.* **240**, 261 (1996).
- ¹⁴N. Tsujii, J. He, K. Yoshimura, K. Kosuge, H. Michor, K. Kreiner, and G. Hilscher, *Phys. Rev. B* **55**, 1032 (1997).
- ¹⁵Z. Fisk, J. D. Thompson, and H. R. Ott, *J. Magn. Magn. Mater.* **76-77**, 637 (1988).
- ¹⁶Z. Fisk and M. B. Maple, *J. Alloys Compd.* **183**, 303 (1992).
- ¹⁷R. Cerny, M. François, K. Yvon, D. Jaccard, E. Walker, V. Petříček, I. Císarová, H-U. Nissen, and R. Wessicken, *J. Phys.: Condens. Matter* **8**, 4485 (1996).
- ¹⁸W. C. Mattens, R. A. Elenbaas, and F. R. de Boer, *Commun. Phys.* **2**, 147 (1977).
- ¹⁹L. C. Gupta, D. E. MacLaughlin, C. Tien, C. Godart, M. A. Edwards, and R. D. Parks, *Phys. Rev. B* **28**, 3673 (1983).
- ²⁰R. Ruzitschka, R. Hauser, E. Bauer, J. G. Soldevilla, J. C. Gomez Sal, K. Yoshimura, N. Tsujii, and K. Kosuge, *Physica B* **230-232**, 279 (1997).
- ²¹M. H. Besnus, J. P. Kappler, P. Lehmann, and A. Meyer, *Solid State Commun.* **55**, 779 (1985).
- ²²H. v. Löhneysen, H. G. Schlager, and A. Schröder, *Physica B* **186-188**, 590 (1993).
- ²³T. Graf, J. M. Lawrence, M. F. Hundley, J. D. Thompson, A. Lacerda, E. Haanappel, M. S. Torikachvili, Z. Fisk, and P. C. Canfield, *Phys. Rev. B* **51**, 15 053 (1995).
- ²⁴A. C. Hewson and J. W. Rasul, *J. Phys. C* **16**, 6799 (1983).
- ²⁵H. Michor *et al.* (unpublished).
- ²⁶C. D. Bredl, S. Horn, F. Steglich, B. Lüthi, and R. M. Martin, *Phys. Rev. Lett.* **52**, 1982 (1984).
- ²⁷T. Fujita, K. Satoh, Y. Onuki, and T. Komatsubara, *J. Magn. Magn. Mater.* **47-48**, 66 (1985).
- ²⁸A. Yoshimori and H. Kasai, *J. Magn. Magn. Mater.* **31-34**, 475 (1983).
- ²⁹M. Lavagna, C. Lacroix, and M. Cyrot, *J. Phys. F* **13**, 1007 (1983).
- ³⁰The values of T_0 of $\text{YbCu}_{5-x}\text{Ag}_x$ estimated from the electronic specific-heat coefficient in Ref. 14 are incorrect by a factor of 0.125. The corrected values of T_0 are 145.1, 129.7, 80.2, 69.3, and 66.2 K, for $x=1.0, 0.85, 0.5, 0.25,$ and $0.125,$ respectively.
- ³¹E. Bauer, R. Hauser, E. Gratz, K. Payer, G. Oomi, and T. Kagayama, *Phys. Rev. B* **48**, 15 873 (1993).
- ³²T. Kagayama and G. Oomi, in *Proceedings of the Hiroshima Workshop on Transport and Thermal Properties of f-electron Systems*, edited by G. Oomi, H. Fujii, and T. Fujita (Plenum, New York, 1993).
- ³³T. Kagayama, G. Oomi, H. Takahashi, N. Mori, Y. Onuki, and T. Komatsubara, *Phys. Rev. B* **44**, 7690 (1991).
- ³⁴J. M. Lawrence, G. H. Kwei, J. L. Sarrao, Z. Fisk, D. Mandrus, and J. D. Thompson, *Phys. Rev. B* **54**, 6011 (1996).
- ³⁵J. He, N. Tsujii, K. Yoshimura, K. Kosuge, and T. Goto, *J. Phys. Soc. Jpn.* **66**, 2801 (1997).